Journal of Visualization, Vol. 2, No. 2 (1999) 153-158

# An Examination of the Flow Induced by the Motion of Many Buoyant Bubbles

Bunner, B.* and Tryggvason, G.*

* Department of Mechanical Engineering and Applied Mechanics, The University of Michigan, Ann Arbor, MI 48109, USA.

Received 17 February 1999.
Revised 15 June 1999.

***Abstract*:** The results of direct numerical simulations of the motion of many three-dimensional buoyant bubbles in periodic domains are examined. The bubble motion is computed by solving the full Navier-Stokes equations by a parallelized finite difference/front tracking method that allows a fully deformable interface between the bubbles and the ambient fluid and the inclusion of surface tension. The governing parameters are selected such that the average rise Reynolds number is about 25. Two cases are examined. In one, the bubbles are nearly spherical; in the other, the bubbles rise with an ellipsoidal shape. The ellipsoidal bubbles show a much larger fluctuation velocity and by visualizing the flow field it is possible to show that the difference is due to larger vorticity generation and stronger interactions of the deformable bubbles. The focus here is on the early stage of the flow, when both the spherical and the deformable bubbles are nearly uniformly distributed.

***Keywords*:** bubbly flows, direct numerical simulations.

## 1. Introduction

While direct numerical simulations have become a standard research tool in the study of the turbulent motion of homogeneous flows, such simulations are more recent for multiphase flows, where the flow field around all particles is fully resolved, inertial and viscous effects are both accounted for, and the phase boundaries are deformable. Direct numerical simulations can provide a complete picture of the flow field in a wide range of volume fractions whereas the amount of measurement points and the maximum volume fraction are limited in experiments. They also provide quantitative data for the development and validation of models used in practical engineering applications such as Reynolds stress, microstructure, and diffusion coefficients.

Due to the challenge of simulating the unsteady motion of moving fluid interfaces, most investigators have made simplifications by, for example, assuming that the bubbles can be represented as point particles (Spelt and Biesheuvel, 1997), or by neglecting inertia (Davis, 1997) or viscosity (Smereka, 1993; Sangani and Didwania, 1993). For bubbles of finite size at finite Reynolds numbers, Ryskin and Leal (1984) and Takagi and Matsumoto (1995) used boundary fitted methods to simulate the rise of a single bubble. While this leads to accurate results, it is limited to the simulation of a single bubble because of the necessity to adapt the grid around the bubble. A volume of fluid (VOF) method was used by Tomiyama et al. (1993) to compute the motion of a single bubble. The VOF method enables to simulate many bubbles, but special techniques must be devised to prevent the bubbles from merging when they come close to each other. Other methods for the calculation of fluid interfaces include the CIP method of Yabe (1997) and the level set method of Sussman, Smereka, and Osher (1994).

In this paper, we use a parallel version (Bunner and Tryggvason, 1999) of a finite difference/front tracking method originally developed by Unverdi and Tryggvason (1992). The interface, or front, between each bubble and the suspending fluid, is tracked explicitly by a moving mesh. The interface is free of contaminants. Bubbles that

are close to each other are not allowed to coalesce, the goal being to obtain statistical results over long periods of time. Absence of contamination and coalescence are difficult to achieve in experiments and the possibility to isolate these effects is another advantage of numerical simulations. In previous studies using this finite difference/front tracking method, Esmaeeli and Tryggvason (1998; 1999) examined the motion of up to 324 bubbles in two dimensions and 8 bubbles in three dimensions in dense homogeneous suspensions. In this paper we examine the results of two three-dimensional simulations of dilute supensions with 27 bubbles. The bubbles, velocity, kinetic energy, and vorticity are displayed using the Advanced Visualization System (AVS) software.

## 2. Results

The results of two simulations are presented here. Both include 27 bubbles at a void fraction of 2% and were performed on a $192^3$ computational grid. There are about 21 grid points across the diameter of one bubble and grid refinement studies have shown that this resolution ensures good accuracy. The Galileo number, $N=\rho^2 g d^3/\mu^3$, is 900 in both cases. The difference is the Eötvös number, $E_o=\rho g d^2/\sigma$, which is 1.0 in the first simulation and 5.0 in the second simulation, corresponding to nearly spherical and ellipsoidal bubbles, respectively. For these parameters, the rise Reynolds number of a single contaminated bubble in an unbounded flow is about 26 for both $E_o=1$ and $E_o=5$ (Clift, Grace, and Weber, 1978). The results are shown until nondimensional time $t=80$, the time being normalized by gravity and the diameter of a bubble. At this time, the bubbles have risen by a distance of about 80 bubble diameters on the average. Each computation was performed on 8 nodes of an IBM SP2 at the University of Michigan and required about 18,000 time steps, each step taking about 130 seconds.

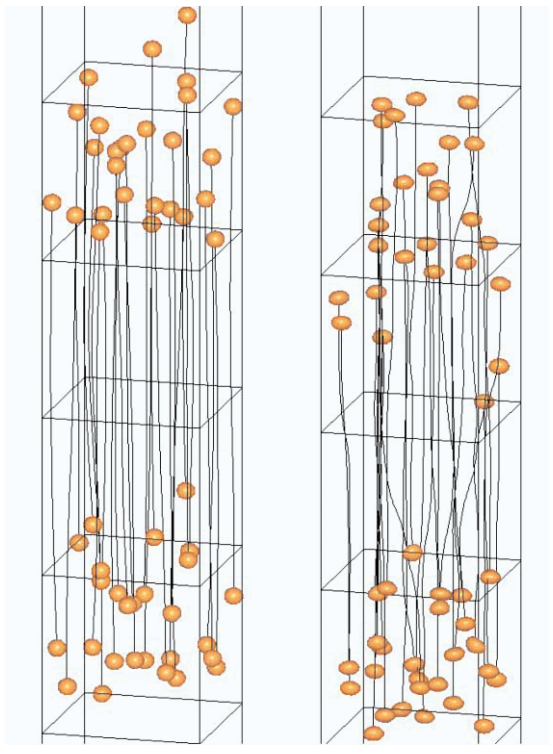

Fig. 1. The 27 bubbles at times 28.6 and 57.2.

In Fig. 1, the 27 nearly spherical bubbles are shown at dimensionless times 28.6 and 57.2, along with the trajectories described by their centroids. The nearly spherical ones ($E_o=1$) are on the left and the ellipsoidal ones ($E_o=5$) are on the right. The flow field (pressure and velocity) is computed in a cubic periodic domain, whose boundaries are outlined by thin lines. In the figure, the domain is reproduced a number of times in the vertical direction. The bubbles are initially inside one domain. As they rise, they move through successive periodic domains and quickly disperse over several periods. Dispersion and path fluctuation are larger for the ellipsoidal bubbles than for the spherical ones. At this void fraction, 2%, the spherical bubbles interact only minimally.

Although they have risen by approximately 55 bubble diameters or 6 periodic boxes, almost all the bubbles are still contained within one periodic box, whereas the ellipsoidal bubbles are spread over 2 periodic boxes.

The average rise velocities are plotted in Fig. 2. The average velocity first approaches the rise Reynolds number of a regular array of bubbles, but as the wakes of the bubbles extend to the bubbles behind, the motion becomes unsteady and the rise Reynolds number decreases. Since the number of bubbles simulated is finite, the rise velocities are not completely steady but fluctuate slightly around average values of 27 ( $E_o$=1) and 26 ( $E_o$=5). The reduction in the rise velocity as the bubble motion becomes unsteady is a finite Renolds number phenomena and has been attributed to increased generation of vorticity by Esmaeeli and Tryggvason (1999).

The average rise velocity fluctuations, or r.m.s. velocities, are plotted in Fig. 3. Although the r.m.s. velocities also fluctuate with time, they reach an approximately statistical steady state. While the rise velocities of the spherical and ellipsoidal bubbles are nearly equal, there is an order of magnitude difference in the fluctuation velocity, explaining the much higher dispersion of the ellipsoidal bubbles.

To obtain more insight into the flow field and to understand the differences between the spherical and deformable bubbles, we plot, in Figs. 4 and 5, the bubbles at time 60, along with streamlines and contour plots of the enstrophy $\bar{\omega}\cdot\bar{\omega}$, where $\bar{\omega}=\nabla\times\bar{U}$, in a vertical plane through the domain. Since the bubbles have moved and are dispersed over more than one periodic domain, at least in the $E_o$=5 case, they are translated back into the original periodic domain, where the velocity is computed. The bubbles which are shaded lie behind the plane of the vorticity contour. High values of vorticity are colored in red and can be observed at the equators of the bubbles and behind them. Considerable differences are observed between the $E_o$=1 and $E_o$=5 cases.

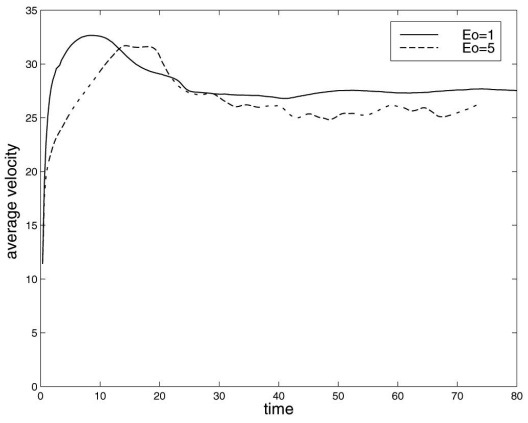


Fig. 2. Average rise Reynolds number.

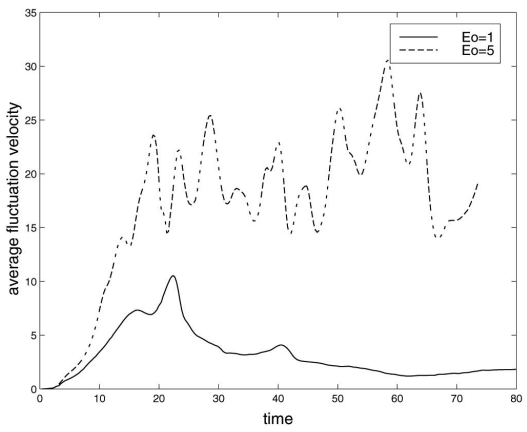


Fig. 3. Average rise velocity fluctuations.

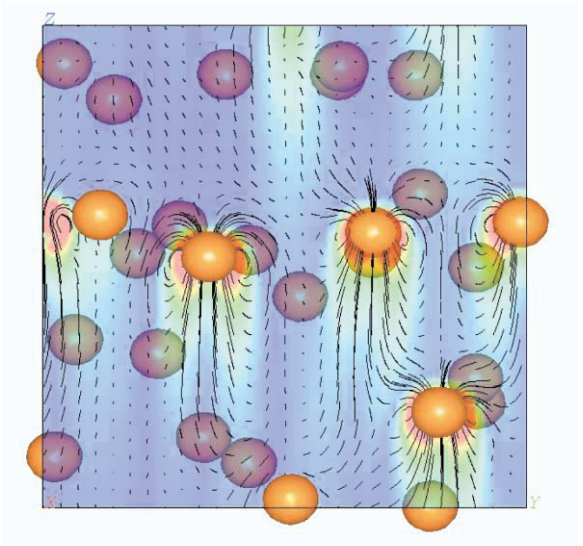

Fig. 4. The 27 spherical bubbles with vorticity contours and streamlines.

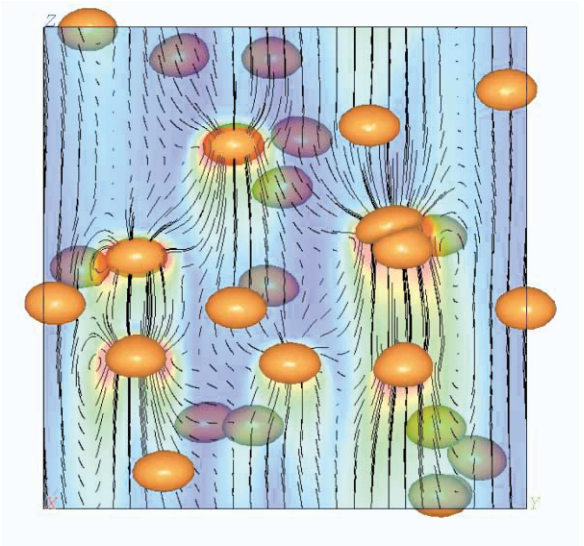

Fig. 5. The 27 ellipsoidal bubbles with vorticity contours and streamlines.

In Fig. 4, four of the five bubbles that are cut by the vorticity plane are aligned horizontally with respect to each other, while the fifth one trails behind. This relates to the observation made in Bunner and Tryggvason (1998) that pairs of spherical bubbles tend to align themselves horizontally. When a bubble is caught in the wake of another bubble, it accelerates at first; both bubbles then rotate around each other and rise in a side-by-side configuration, where they move away from each other until they reach an equilibrium position. This is the "drafting, kissing, and tumbling" mechanism mentioned by Fortes, Joseph, and Lundgren (1987).

While we believe this mechanism still applies to the deformable bubbles, in the general case, there are major differences. On the right side of Fig. 5, two bubbles are undergoing collision, while a third one is trailing in their wake. This section of the flow field is shown in more detail in Fig. 6. A region of high vorticity and velocity linking the three bubbles is clearly observable. The shapes of these three bubbles are also very different from that seen in quieter sections of the flow. The top bubble is flatter because it is pushed by the one below; the upper side of the bottom bubble is deformed as it is sucked into the wake. This pairing process is repeated periodically as the bubbles rise.

If the two top bubbles of Fig. 6 were alone in an unbounded flow, they would also tumble and eventually move away from each other into a side-by-side configuration. The beginning of this tumbling motion can be seen. However, due to the presence of other bubbles, more complex interactions, including more than two bubbles, are possible, see for example the formation of the stream in Fig. 6. Since the flow is homogeneous, the bubbles are on the average oriented such that the angle between their major axis and the vertical direction is 90 degrees. This angle exhibits high-frequency oscillations with an amplitude of up to 40% corresponding to the tumbling of bubbles about each other.

A detail of Fig. 4 is shown in Fig. 7. Although the bubbles are close, their vorticity contours do not intersect. The limited interaction of spherical bubbles can also be observed by looking at isosurfaces of the kinetic energy, in Fig. 8 for $E_o$=1, and Fig. 9 for $E_o$=5. Both plots are for the same value of the kinetic energy, defined here as $E=(1/2)\bar{U}\cdot\bar{U}$. The isosurfaces behind the ellipsoidal bubbles extend farther than the ones behind spherical bubbles, which are confined close to the bubble surface. Consequently, the spherical bubbles have less power to draft trailing bubbles in their wake, especially at a low void fraction. For ellipsoidal bubbles, the formation of a high-velocity "tube" or "stream" around the three bubbles is seen on the right side of Fig. 9.

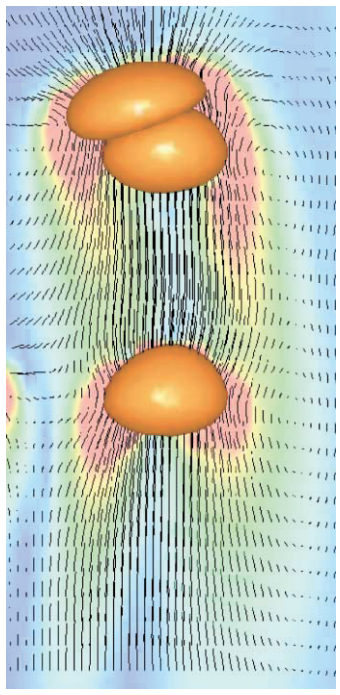

Fig. 6. Detail of the 27 ellipsoidal bubbles.

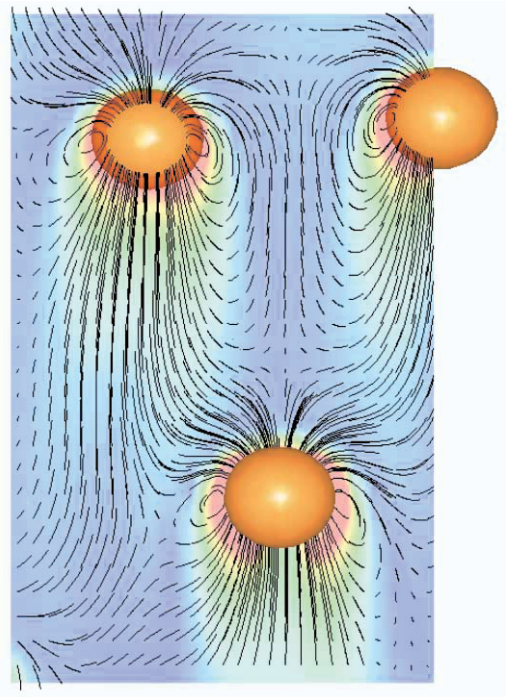

Fig. 7. Detail of the 27 spherical bubbles.

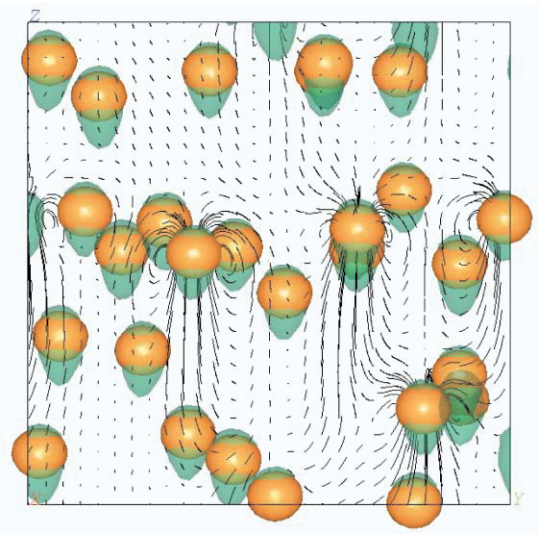

Fig. 8. The 27 spherical bubbles with a kinetic energy isosurface and streamlines.

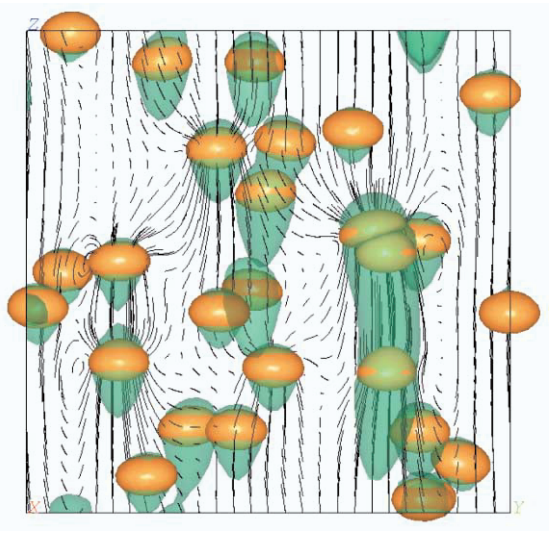

Fig. 9. The 27 ellipsodial bubbles with a kinetic energy isosurface and streamlines.

## 3. Conclusion

Three-dimensional flow visualization can provide considerable insight into the dynamics of buoyant bubbly flows. This helps in developing an understanding of the driving mechanisms and in the formulation of hypotheses for further studies. Two systems, for which the surface tension was the only difference, were examined. Although a single spherical and ellipsoidal bubble behave similarly in an unbounded flow and the average rise velocity of the 27 bubbles is approximately the same, the visualization shows that there are considerable differences in the way the bubbles interact. The spherical bubbles stay away from each other, but the ellipsoidal bubbles form streams, in which the bubbles rise faster than surrounding bubbles. These streams are not stable but break up, so that the average rise velocity is approximately the same as that of the spherical bubbles. One consequence is much higher fluctuation velocities. A more extensive analysis of these flows, including a discussion of the mechanisms leading to the formation of stable streams of deformable bubbles at later stages of the flow, will be published later.

In addition to this examination of the flow field at several times, AVS has been used to generate movies to capture the unsteady nature of the flow. A few of these movies are available on the homepage of the first author at http://www-personal.engin.umich.edu/~bunner/. This work was supported by the National Science Foundation under grant CTS-9503208 and by a Rackham fellowship from the University of Michigan. The computations were performed at the Center for Parallel Computing at the University of Michigan through NPACI and at the Maui High Performance Computing Center through NCSA.

### *References*

Bunner, B. and Tryggvason, G., Direct Numerical Simulation of Large Three-Dimensional Bubble Systems, Proceedings of the 1998 A SME Fluids Engineering Division Summer Meeting (Washington), June 1998.

Bunner, B. and Tryggvason, G., A parallel front-tracking method for the simulation of dispersed multiphase flows, Proceedings of the Ninth SIAM Conference on Parallel Processing for Scientific Computing (San Antonio), March 1999.

Clift, R., Grace, J. R., and Weber, M. E., Bubbles, Drops, and Particles, (1978), Academic Press.

Davis, R. H., Buoyancy-driven viscous interaction of a rising drop with a smaller trailing drop, Physics of Fluids, 11-5 (1999), 1016-1028.

Esmaeeli, A. and Tryggvason, G., Direct numerical simulations of bubbly flows. Part I-Low Reynolds number arrays, J. Fluid Mech ., 377 (1998), 313-345.

Esmaeeli, A. and Tryggvason, G., Direct numerical simulations of bubbly flows. Part II-Moderate Reynolds number arrays, J. Flui d Mech., 385 (1999), 325-358.

Fortes, A., Joseph, D. D., and Lundgren, T., Nonlinear mechanics of fluidization of beds of spherical particles, J. Fluid Mech. , 177 (1987), 467-483.

Ryskin, G. and Leal, L. G., Numerical solution of free-boundary problems in fluid mechanics, Part 1., The finite-difference tec hnique, J. Fluid. Mech., 148 (1984), 1-17.

Sangani, A. S. and Didwania, A. K., Dynamic simulations of bubbly liquids at large Reynolds numbers, J. Fluid. Mech., 250 (1993), 307-337.

Smereka, P., On the motion of bubbles in a periodic box, J. Fluid Mech., 254 (1993), 79-112.

Spelt, P. D. M. and Biesheuvel, A., On the motion of gas bubbles in homogeneous isotropic turbulence, J. Fluid. Mech., 336, (1997), 221-244.
Sussman, M., Smereka, P., Osher, S., A level set approach for computing solutions to incompressible two-phase flows, J. Comput. Phys., 114 (1994), 146-159.
Takagi, S. and Matsumoto, Y., Three dimensional calculation of a rising bubble, Proceedings of the Second International Confere nce on Multiphase Flows (Tokyo), (1995).
Tomiyama, A., Sou, A., Minagawa, H., and Sakaguchi, T., Numerical analysis of a single bubble by VOF method, JSME International Journal, 36 (1993), 51-55.
Unverdi, S. O. and Tryggvason, G., A front-tracking method for viscous, incompressible, multi-fluid flows, J. Comput. Phys., 100 (1992), 25-37.
Yabe, T., Unified solver CIP for solid, liquid, and gas, Computational Fluid Dynamics Review (1997).

## *Authors' Profiles*

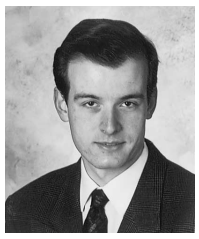

Bernard Bunner: He is a doctoral candidate in the Department of Mechanical Engineering and Applied Mechanics at the University of Michigan. After his undergraduate education at E.N.S.T.A. in Paris, France, and at the University of Aachen, Germany, he worked in industry for one year before joining the group of Professor Tryggvason. His thesis topic is the direct numerical simulation of bubbly flows. His research interests are in computational fluid dynamics, multiphase flows, and parallel computing. He also obtained a master's degree in electrical engineering with a focus on digital communications.

Gretar Tryggvason: He received his Ph.D. from Brown University and joined the Department of Mechanical Engineering and Applied Mechanics at the University of Michigan in 1985 after a year as a research scientist at the Courant Institute. He is an active member in several professional societies and an Associate Editor of the Journal of Computational Physics. His research interests include multiphase and free surface flows, vortex flows and combustion, phase changes, solidification, and numerical methods.